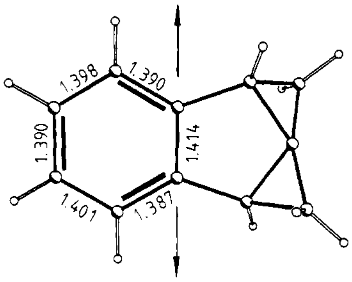

Figure 4.

annulated bond (1.414 Å) and to alternate the distances of the other C–C bonds (1.390, 1.398, 1.390, 1.401, 1.387) leaning toward *one* Kekulé structure (Figure 4).

The X–X electron density distribution (Figure 3) reveal no distortion by a shift of the maxima from the direct atom linkages in the benzene ring, as could be shown by annulation of small-membered rings.[11] Within the five-membered ring the maxima are shifted exocyclic of the bonds C3–C4 and C5–C6, respectively, indicative of the tension of the spring spiropentane.[17]

In tricyclo[2.1.0.0^{1,3}]pentane[18] containing a *zero* bridge between C3–C4 or C2–C5, respectively, bonding and twisting of spiropentane (**1**) comes to an extreme. Here the calculated exocyclic angle at the spiroatom exceeds linearity to 193.91°, thus leading to an inverted carbon.

Acknowledgment. Work at the Ruhr-Universität was generously supported by the Deutsche Forschungsgemeinschaft (Br 667/4-5) and the Fonds der Chemischen Industrie.

Supplementary Material Available: Tables of atomic positional parameters and complete listings of bond angles and bond distances of **1**, **2**, and **3** (13 pages); tables of observed and calculated structure factors (61 pages). Ordering information is given on any current masthead page.

---

[17] Because of the twisting of the five-membered rings the sections of the bonds mentioned are not exactly within the plane shown in Figure 3. Planes exactly through the atoms cited show the same tendency toward exocyclic shifts.

[18] Wiberg, K. B.; McClusky, J. V. *Tetrahedron Lett.* **1987**, *28*, 5411.

(Binaphtholate)$\mathrm{W_2(O\text{-}\mathit{t}\text{-}Bu)_4}$: The First Metal–Metal Multiple Bond Supported by a Chiral Alkoxide Ligand

Joseph A. Heppert,*,[1a] Steven D. Dietz,[1a] Timothy J. Boyle,[1a] and Fusao Takusagawa[1b]

Department of Chemistry, University of Kansas
Lawrence, Kansas 66045

Received October 21, 1988

Functionalized binaphthyl subunits are useful templates for controlling the stereochemistry of macrocycles, transition-metal complexes, and main-group hydride reagents.[2-5] Nyori has demonstrated that binaphtholate ligands are particularly useful chiral auxiliaries for alane-reducing agents in stereospecific reactions with ketones.[5] Despite the demonstrated utility of main-group binaphtholate complexes in enantiospecific synthesis and probable suitability of binaphtholate substituents as ligands for high valent transition metals, extremely few studies of the coordination chemistry of binaphtholates with transition metals have been forthcoming.[3] We now report the syntheses of (3,3′-$\mathrm{R_2}$-1,1′-bi-2,2′-naphtholate)$\mathrm{W_2(O\text{-}\mathit{t}\text{-}Bu)_4}$ molecules, the first examples of the "$\mathrm{W_2(OR)_6}$" class of metal–metal multiple bonds containing a chiral-supporting alkoxide ligand. To our knowledge, this is the first report of a structurally characterized binaphtholate derivative of a dinuclear transition-metal complex and is representative of a potentially wide-ranging class of easily accessible early transition-metal complexes rendered chiral by this type of supporting ligand.

A toluene solution of 3,3′-dimethylbinaphthol (DMBINOH),[2b] dried over 5 Å molecular sieves, was slowly added to a solution of $\mathrm{W_2(O\text{-}\mathit{t}\text{-}Bu)_6}$[6] in toluene at 0 °C. After 2 h, the solvent was removed in vacuo, and the solid residue was extracted repeatedly with neat toluene. Two recrystallizations from toluene resulted in the isolation of (3,3′-$\mathrm{Me_2}$-1,1′-{2-$\mathrm{OC_{10}H_5}$}$_2$)$\mathrm{W_2(O\text{-}\mathit{t}\text{-}Bu)_4}$ as nearly equidimensional orange-brown cubes in 55% yield.[7] The analogous (1,1′-{2-$\mathrm{OC_{10}H_5}$}$_2$)$\mathrm{W_2(O\text{-}\mathit{t}\text{-}Bu)_4}$ product was purified by recrystallization from hexanes. Both products are extremely air and moisture sensitive, decomposing over a few hours in the solid state after exposure to moist air. The ^{1}H NMR spectra of the complexes (Figure 1) are invariant over a wide temperature range (50 °C through −50 °C) and suggest that the molecule possesses rigorous C_2 symmetry in solution.

The molecular structure of (DMBINO)$\mathrm{W_2(O\text{-}\mathit{t}\text{-}Bu)_4}$, shown in the ball and stick representations in Figure 2,[8] demonstrates that the molecule has a monomeric $\mathrm{W_2(OR)_6}$-type framework consistent with the spectroscopic data. The W–W distance of 2.324 (1) Å is within the normal range observed for homoleptic

---

[1] (a) Department of Chemistry. (b) X-ray Crystallographic Laboratory, Department of Chemistry.

[2] (a) Cram, D. J.; Helgeson, R. C.; Peacock, S. C.; Kaplan, L. J.; Domeier, L.; Morgan, P.; Koga, K.; Mayer, J. M.; Chao, Y.; Siegel, M. G.; Hoffman, D. H.; Sogah, G. D. Y. *J. Org. Chem.* **1978**, *43*, 1930. (b) Lingfelter, D. S.; Helgeson, R. C.; Cram, D. J. *J. Org. Chem.* **1981**, *46*, 393.

[3] (a) Olivero, A. G.; Weldmann, B.; Seebach, D. *Helv. Chim. Acta* **1981**, *64*, 2485. (b) Seebach, D.; Beck, A. K.; Roggo, S.; Wonnacott, A. *Chem. Ber.* **1985**, *118*, 3673. (c) Schnutenhaus, H.; Brintzinger, H. H. *Angew. Chem., Int. Ed. Engl.* **1979**, *18*, 777. (d) Wild, F. R. W. P.; Zsolnai, L.; Huttner, G.; Brintzinger, H. H. *J. Organomet. Chem.* **1982**, *232*, 233.

[4] (a) Kitamura, M.; Hisao, Y.; Nyori, R.; Takaya, H. *Tetrahedron Lett.* **1987**, *28*, 4829. (b) Ikariya, T.; Ishii, Y.; Kawano, H.; Arai, T.; Sabari, M.; Yoshikawa, S.; Akutagawa, S. *J. Chem. Soc., Chem. Commun.* **1985**, 927. (c) Ohta, T.; Takaya, H.; Kitamura, M.; Nagai, K.; Nyori, R. *J. Org. Chem.* **1987**, *52*, 3174. (d) Ohta, T.; Takaya, H.; Nyori, R. *Inorg. Chem.* **1988**, *27*, 566.

[5] (a) Nyori, R.; Tomino, I.; Tanimoto, Y. *J. Am. Chem. Soc.* **1979**, *101*, 3129. (b) Nyori, R. *Pure Appl. Chem.* **1981**, *53*, 2315.

[6] (a) Schrock, R. R.; Listeman, M. L.; Sturgeoff, L. G. *J. Am. Chem. Soc.* **1982**, *104*, 4291. (b) Sharp, P. R.; Schrock, R. R. *J. Am. Chem. Soc.* **1980**, *102*, 1430.

[7] 3,3′-Dimethyl-1,1′-bi-2,2′-naphthol (0.50 g) and $\mathrm{W_2(O\text{-}\mathit{t}\text{-}Bu)_6}$ (1.28 g) yielded crystalline (3,3′-dimethyl-1,1′-bi-2,2′-naphtholate)$\mathrm{W_2(O\text{-}\mathit{t}\text{-}Bu)_4}$ (0.85 g) for an overall 55% yield. Analytical data: ^{1}H NMR spectrum (benzene-d_6, 20 °C) $\delta = 7.83$ (2 H, s, *NAP*($H_{4,4'}$)), 7.79, 7.38 (2 H, d, $J = 8.3$ Hz, *NAP*($H_{5,5'}$ *and* $H_{8,8'}$)), 7.17, 6.95 (2 H, t, $J = 8.3$ Hz, *NAP*($H_{6,6'}$ *and* $H_{7,7'}$)), 2.88 (6 H, s, *3,3′-Me*$_2$), 1.75, 0.67 (18 H, s O-*t-Bu*); ^{13}C NMR spectrum (benzene-d_6, 18 °C) $\delta = 167.1$ (*NAP* ($C_{2,2'}$)), 134.0, 130.8, 130.4, 128.9, 127.1, 176.4, 125.6, 124.2, 121.6 (*NAP*), 83.6, 75.2 (O*C*Me$_3$), 35.6, 32.3 (OC*Me*$_3$), 18.8 (*Me*). Anal. data calcd, C = 46.91, H = 5.43; found, C = 47.16, H = 5.37.

[8] Crystal data for (3,3′-dimethyl-1,1′-bi-2,2′-naphtholate)$\mathrm{W_2(O\text{-}\mathit{t}\text{-}Bu)_4}$ [(DMBINO)$\mathrm{W_2(O\text{-}\mathit{t}\text{-}Bu)_4}$]: An orange crystal (~0.1 × 0.1 × 0.1 mm) obtained by recrystallization from toluene was glued onto a glass fiber and mounted on a Syntex P2$_1$ diffractometer equipped with a LT-1 low-temperature device. The X-ray experiments were carried out with Cu Kα radiation ($\lambda = 1.5418$ Å) at −120 °C in order to avoid decomposition of the crystal by moisture and oxygen. The crystal data were as follows: space group $Pna2_1$; cell dimensions, $a = 22.745$ (3) Å, $b = 12.398$ (3) Å, $c = 13.150$ (3) Å; $Z = 4$; $D_{\mathrm{calcd}} = 1.750$ g/cm^3. Another possible space group, *Pnam*, was excluded by inspection of a Patterson map, and the space group $Pna2_1$ was confirmed by a successful structure refinement. Reflections (4215) were measured up to $\sin\theta/\lambda = 0.50$, and the intensities were corrected for absorption, decay, Lorentz and polarization effects. Independent reflections (2011) were obtained by merging equivalent reflections. R_{int} for merging was 0.043. All of the reflections were used in the structure determination and refinements. The positions of two crystallographically independent tungsten atoms were determined by the interpretation of a Patterson map. Successive difference Fourier syntheses revealed the positions of all of the carbon and oxygen atoms. The structure was refined by a full-matrix least-squares method by using anisotropic thermal parameters for tungsten atoms and isotropic thermal parameters for carbon and oxygen atoms. The function minimized was $\sum w(|F_o| - |F_c|)^2$ with $w = 1/\sigma(F_o)^2$. Refinement was converged to $R = 0.044$, $R_w = 0.051$, $S = 0.948$ for all data. Although the R factor was reduced from 0.0441 to 0.0439 when all of the atoms were anisotropically refined, several thermal parameters became nonpositively defined. Thus, all oxygen and carbon atoms were isotropically refined. The final difference map did not show any significant electron density for the hydrogen atoms and displayed no significant residuals in unexplained positions. Atomic scattering factors including an anomalous dispersion correction factor for the tungsten atoms were taken from *International Tables for X-ray Crystallography*, 1974.

0002-7863/89/1511-1503$01.50/0

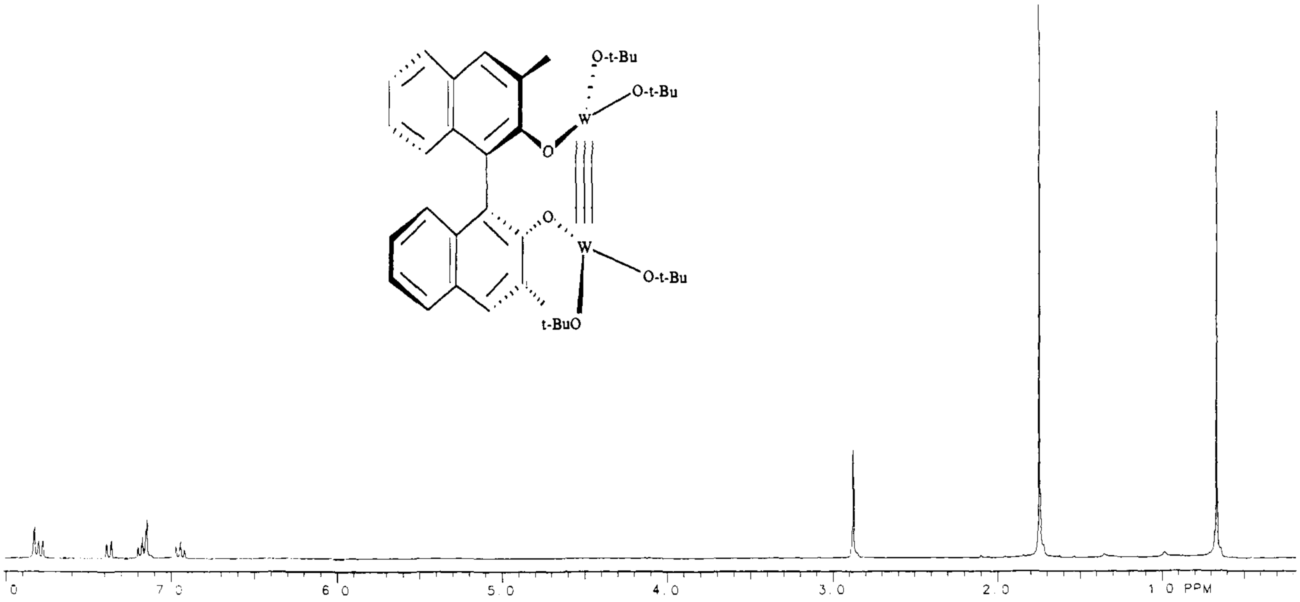

Figure 1. 300 MHz ^1H NMR spectrum of (DMBINO)W_2(O-*t*-Bu)$_4$.

$W_2(OR)_6$ molecules.[9] A view of the molecule perpendicular to the W–W bond vector (Figure 2b) clearly shows the binaphtholate to be a bridging ligand which imposes virtual C_2 symmetry on the molecule. The C(10)–C(21) attachment of the two naphthalene units is only slightly skewed from being exactly perpendicular to the W–W bond vector, while the approximate 90° dihedral angle described by the two naphthalene rings is greater than the 65–75° angle observed in the structures of mononuclear complexes that contain a 1,1′-BINAP ligand.[4d,10] The view down the W–W axis (Figure 2a) demonstrates that the (DMBINO)W_2(O-*t*-Bu)$_4$ retains its staggered ethane-like geometry, with the binaphthyl linkage enforcing a gauche arrangement of the naphthol units. The view down the pseudo-3-fold axis of the molecule suggests that the two alkoxide ligands proximal to the naphtholate units should be in the shielding cone of the aromatic rings.

A study of the shielding influence of the binaphtholate ligand on the O-*t*-Bu ligands provides support for the similarity of the molecular structure in both solution and the solid phase. The ^1H NMR spectrum of (DMBINO)W_2(O-*t*-Bu)$_4$ shows two strangely disparate environments for the O-*t*-Bu ligands, with one appearing at $\delta = 0.68$. By inference, this resonance represents the O-*t*-Bu groups crowded into the space under the naphthalene rings. NOE difference ^1H NMR spectroscopy shows only modest energy transfer between the O-*t*-Bu groups and the hydrogens of the naphthalene ring, with the most significant effect being the C_4 naphthalene singlet at $\delta = 7.83$ during irradiation of the O-*t*-Bu resonance at $\delta = 0.68$. This observation lends some support for the proximity of the naphthalene rings to the unusually shifted O-*t*-Bu units. The UV–vis spectra of the products contain three major bands at 235, 278, and 332 nm (ϵ = > 80 000, 23 000, and 12 000, respectively) consistent with the expected major exciton absorbance and E-band absorbance of the binaphtholate ligands, respectively. A shoulder on the 332-nm band that tails into the visible region is consistent with the $\pi \rightarrow \pi^*$ transition observed in homoleptic $W_2(OR)_6$ complexes, and a corresponding weak $(\pi \rightarrow \pi^*)^3$ transition is barely visible at 421 nm ($\epsilon \leq 1800$).[11]

The (*R*)-(2,2′-bi-1,1′-naphthol)W_2(O-*t*-Bu)$_4$ complex prepared from (*R*)-2,2′-bi-1,1′-naphthol ((*R*)-BINOH) displayed a rotation of $[\alpha]_n^{20} = 32.4°$. The CD spectrum of ((*R*)-BINO)W_2(O-*t*-Bu)$_4$ shows bands with positive Cotton effects at 326 and 350 nm representing the E-band and magnetically allowed component of the $\pi \rightarrow \pi^*$ transitions observed in the UV–vis spectrum of the

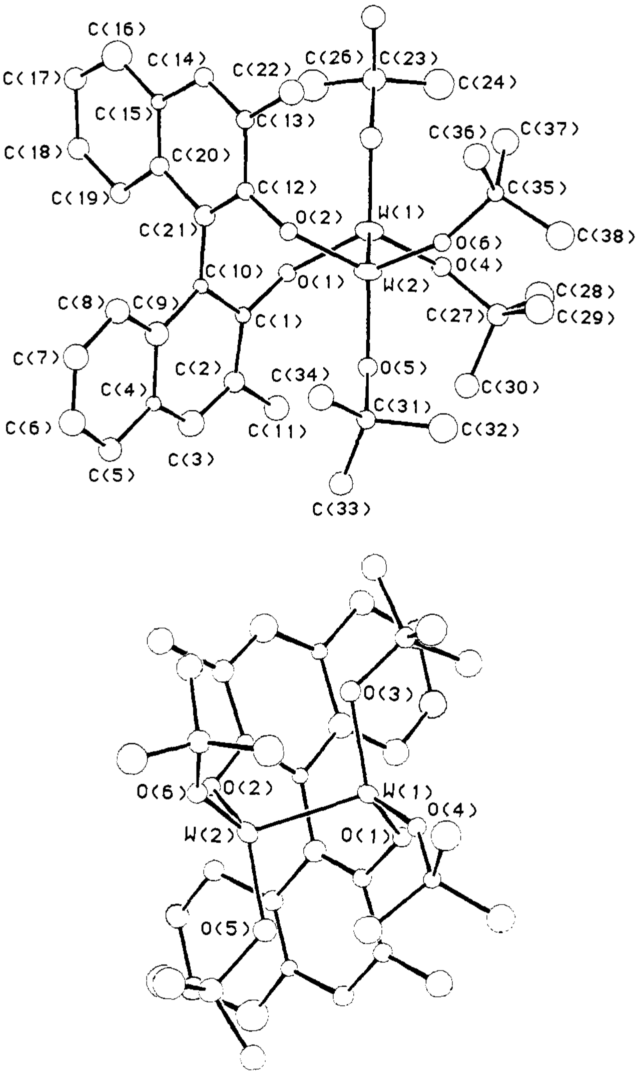

Figure 2. Ball and stick representations of the structure of (DMBINO)W_2(O-*t*-Bu)$_4$ viewed (A, top) down the W–W bond axis and (B, bottom) perpendicular to the W–W and C_{10}–C_{21} (naphthalene-to-naphthalene) bond axes.

---

(9) Chisholm, M. H.; Folting, K.; Hampden-Smith, M.; Smith, C. A. *Polyhedron* **1987**, *6*, 1747.

(10) Toriumi, K.; Ito, T.; Takaya, H.; Souchi, T.; Nyori, R. *Acta Crystallogr., Sect. B: Struct. Crystallogr. Chem.* **1982**, *B38*, 807.

(11) Chisholm, M. H.; Clark, D. L.; Kober, E. M.; Van Der Sluys, W. G. *Polyhedron* **1987**, *6*, 723.

complex, with an intense exciton-derived CD absorption consistent with retention of the *R* configuration of the binaphtholate ligand at 231 nm.

The new (binaphtholate)W_2(O-*t*-Bu)$_4$ complexes react readily with acetylenes and other unsaturated organic substrates, and studies of the structures of these products and stereoselectivity of the reactions are currently under investigation.

Acknowledgment. We thank Research Corporation for a Cottrell Research Grant and The University of Kansas General Research Fund for support. J.A.H. thanks Dr. J. C. Huffman and Dr. K. Folting for helpful discussions and Prof. A. W. Burgstahler for helpful discussions concerning CD/ORD spectroscopy. S.D.D. acknowledges Dr. D. Vander Velde for helpful discussions regarding NOE spectroscopy.

Supplementary Material Available: Tables of fractional coordinates and isotropic thermal parameters, anisotropic thermal parameters, bond distances, and bond angles and a summary of crystallographic data for 1,2-[3,3′-Me_2-1,1′-$(OC_{10}H_5)_2$]W_2(O-*t*-Bu)$_4$ (8 pages); table of observed and calculated structure factors (12 pages). Ordering information is given on any current masthead page.

Correlation between the Optical Transitions and Metal–Metal Vibrational Frequencies in Pt_4^{9+} Cations: A Resonance Raman Study

Hans K. Mahtani[1] and Paul Stein*

Department of Chemistry, Duquesne University
Pittsburgh, Pennsylvania 15282

Received September 21, 1988

Mixed-valent-state platinum and dinuclear Pt^{III} complexes with bridging amidate ligands have been reported at an accelerated pace.[2-6] Their Pt–Pt bonding continues to attract attention.[7] Three mixed-valent-state platinum complexes have been characterized by X-ray crystallography and shown to contain structurally similar Pt_4^{9+} cations. The *cis*-diammineplatinum α-pyridone blue cation,[4] $Pt_4(NH_3)_8(C_5H_4NO)_4^{5+}$ (**1**), and the *cis*-diammineplatinum 1-methyluracil blue cation,[5] $Pt_4(NH_3)_8(C_5H_5N_2O_2)_4^{5+}$ (**2**), consist of two amidate-bridged dimers of *cis*-diammineplatinum with the exocyclic oxygens coordinated to the inner platinum atoms, Pt2 and Pt2′, as schematically shown:

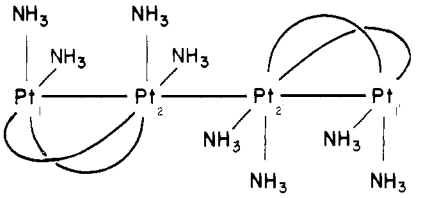

The (ethylenediamine)platinum α-pyridone blue cation, $Pt_4(en)_4(C_5H_4NO)_4^{5+}$ (**3**), is similar to **1**, with *cis*-diammine replaced by ethylenediamine (en) ligands.[6] In this communication we present resonance Raman (rR) spectra of the Pt_4^{9+} cations in aqueous solution and establish a relationship between the two principal optical absorptions and the Pt-Pt vibrational frequencies. The results provide a benchmark for the study of similar platinum clusters, such as the platinum pyrimidine blues.[8]

The rR spectrum of **1** consists of two intense bands due to an interdimer Pt–Pt stretch, ν(Pt2–Pt2′) = 69 cm^{-1}, and an intradimer Pt–Pt stretch, ν(Pt1–Pt2) = 149 cm^{-1}.[9] ν(Pt2–Pt2′) results from the oscillation between the two dimer units as a whole and is a measure of the Pt2–Pt2′ bonding (with an estimated force constant for 0.4 ± 0.1 mdyn/Å) as well as N–H···O interdimer hydrogen bonding. ν(Pt1–Pt2), which contains a significant contribution from the bridging α-pyridonate ligands, is comparable with ν(Pt–Pt) = 170–184 cm^{-1}, observed for bis(*cis*-diammineplatinum(III)) complexes with two bridging α-pyridonate ligands, and ν(Pt–Pt) = 140 cm^{-1}, observed for a corresponding diplatinum(II) complex.[12] The good inverse correlation of the Pt–Pt distances, 2.53–2.57 Å[3c,d] for Pt^{III}_2, 2.89 Å[13] for Pt^{II}_2 complexes, and 2.774 Å for Pt1–Pt2 in **1**, with ν(Pt–Pt) confirms the assignment of ν(Pt1–Pt2). A bond order of 0.2 is estimated for Pt1–Pt2 from ν(Pt–Pt) assuming bond orders of 1 and 0 for the Pt^{III}_2 and Pt^{II}_2 complexes, respectively. Thus the Pt2–Pt2′ and Pt1–Pt2 bonding is nearly equivalent and consistent with previous reports[14,15] that the unpaired electron in **1** is delocalized over the Pt_4^{9+} chain.[16] A structurally similar Pt_4^{10+} cation, *cis*-diammineplatinum α-pyrrolidone tan, shows a rR spectrum[17] having

---

[1] Present address: Dartmouth-Hitchcock Medical Center, Hanover, NH 03756.

[2] (a) Micklitz, W.; Riede, J.; Huber, B.; Müller, G.; Lippert, B. *Inorg. Chem.* **1988**, *27*, 1979. (b) Matsumoto, K.; Takahashi, H.; Fuwa, K. *Ibid.* **1983**, *22*, 4086. (c) Lippert, B.; Schöllhorn, H.; Thewalt, U. *Ibid.* **1987**, *26*, 1736. (d) Matsumoto, K. *Bull. Chem. Soc. Jpn.* **1985**, *58*, 651. (e) Matsumoto, K.; Takahashi, H., Fuwa, K. *J. Am. Chem. Soc.* **1984**, *106*, 2049. (f) Laurent, J.-P.; Legape, P.; Dahan, F. *Ibid.* **1982**, *104*, 7335.

[3] (a) Lippert, B.; Schöllhorn, H.; Thewalt, U. *J. Am. Chem. Soc.* **1986**, *108*, 525. (b) Goodgame, D. M. L.; Rollins, R. W.; Skapski, A. C. *Inorg. Chim. Acta* **1984**, *83*, L11. (c) Hollis, L. S.; Roberts, M. M.; Lippard, S. J. *Inorg. Chem.* **1983**, *22*, 3637. (d) Hollis, L. S.; Lippard, S. J. *Ibid.* **1983**, *22*, 2605. For recent reviews of Pt^{III} binuclear complexes, see: (e) Zipp, A. P. *Coord. Chem. Rev.* **1988**, *84*, 47. (f) Woolins, J. D.; Kelly, P. F. *Ibid.* **1985**, *64*, 115. (g) Cotton, F. A.; Walton, R. A. *Struct. Bonding (Berlin)* **1985**, *62*, 1. (h) O'Halloran, T. V.; Lippard, S. J. *Isr. J. Chem.* **1985**, *25*, 130.

[4] (a) Barton, J. K.; Rabinowitz, H. N.; Szalda, D. J.; Lippard, S. J. *J. Am. Chem. Soc.* **1977**, *99*, 2827. (b) Barton, J. K.; Szalda, D. J.; Rabinowitz, H. N.; Waszczak, J. V.; Lippard, S. J. *Ibid.* **1979**, *101*, 1434.

[5] Mascharak, P. K.; Williams, I. D.; Lippard, S. J. *J. Am. Chem. Soc.* **1984**, *106*, 6428.

[6] O'Halloran, T. V.; Roberts, M. M.; Lippard, S. J. *J. Am. Chem. Soc.* **1984**, *106*, 6427.

[7] (a) Che, C.-M.; Lee, W.-M.; Mak, T. C. V.; Gray, H. B. *J. Am. Chem. Soc.* **1986**, *108*, 4446. (b) Miskowski, V. M.; Gray, H. B. *Inorg. Chem.* **1987**, *26*, 1108.

[8] (a) Davidson, J. P.; Faber, P. J.; Fischer, R. G., Jr.; Mansy, S.; Peresie, H. J.; Rosenberg, B.; Van Camp, L. *Cancer Chemother. Rep.* **1975**, *59*, 287. (b) Flynn, C. M., Jr.; Viswanathan, T. S.; Martin, R. B. *J. Inorg. Nucl. Chem.* **1977**, *39*, 437. (c) Teo, B.-K.; Kijima, K.; Bau, R. *J. Am. Chem. Soc.* **1978**, *100*, 621. (d) Lippert, B. *J. Clin. Hematol. Oncol.* **1977**, *7*, 26. (e) Zaki, A. A.; McAuliffe, C. A.; Friedman, M. E.; Hill, W. E.; Kohl, H. H. *Inorg. Chim. Acta* **1983**, *69*, 93. (f) Woollins, J. D.; Rosenberg, B. *Inorg. Chem.* **1982**, *21*, 1280.

[9] The rR experiments were performed with a 1404 Spex monochromator, a Spectra-Physics 165 krypton ion laser, and an IBM 9000 microcomputer. Data were digitally collected at 0.5-cm^{-1} increments. The rR spectra were obtained by flowing the sample solution through a 1-mm glass capillary tube with a peristaltic pump and silicone tubing. A reservoir was installed in the loop where the samples were maintained near 0 °C using an ice bath. The Pt_4^{9+} samples were verified by their optical absorption spectra, which were typically measured before and after the rR experiments.

[10] Neuberger, D.; Lippert, B. *J. Am. Chem. Soc.* **1982**, *104*, 6596.

[11] Stein, P.; Dickson, M. K.; Roundhill, D. M. *J. Am. Chem. Soc.* **1983**, *105*, 3489.

[12] (a) Mahtani, H. K.; Stein, P. *Proc. XIth Int. Conf. Raman Spectrosc.*; Clark, R. J. H., Long, D. A., Eds.; Wiley: New York, 1988; pp 311–312. (b) Mahtani, H. K.; Black, I.; Stein, P., manuscript in preparation.

[13] Hollis, L. S.; Lippard, S. J. *J. Am. Chem. Soc.* **1983**, *105*, 3494.

[14] Barton, J. K.; Caravana, C.; Lippard, S. J. *J. Am. Chem. Soc.* **1979**, *101*, 7269.

[15] Barton, J. K.; Best, S. A.; Lippard, S. J.; Walton, R. A. *J. Am. Chem. Soc.* **1978**, *100*, 3785.

[16] The rR band widths of ν(Pt2–Pt2′) (~13 cm^{-1}) and ν(Pt1–Pt2) (~18 cm^{-1}) are large compared with those of ν(Pt–Pt) (~5 cm^{-1}) observed for Pt^{II} and Pt^{III} binuclear complexes with bridging μ-pyrophosphito ligands.[11] The line broadening is attributed to a statistical disorder arising from fluctuations in the positions of the coordinating ligands and to shallow potential surfaces along the Pt–Pt normal coordinates. The present observation of a single Raman band for Pt1–Pt2 and Pt1′–Pt2′ stretching is consistent with delocalization of the unpaired electron (i.e., $[Pt^{2.25}]_4$). A localized electron hole (i.e., $Pt^{III}[Pt^{II}]_3$) is expected to exhibit a splitting in ν(Pt1–Pt2) of ~20 cm^{-1} if the hopping frequency is slower than 10^{-12} s. When **1** was prepared by using ClO_4^- in place of NO_3^- anions, we observed low-energy shoulders for ν(Pt2–Pt2′) and ν(Pt1–Pt2). This reproducible observation is attributed to weak coordination of the ClO_4^- anions and not to the onset of a localized electron hole.

0002-7863/89/1511-1505$01.50/0